Available online at www.sciencedirect.com
ScienceDirect
Ceramics International 38S (2012) S339–S342
CERAMICS INTERNATIONAL
www.elsevier.com/locate/ceramint

Electrical properties of $[Li_{0.04}(K_{0.5}Na_{0.5})_{0.96-x}Ag_x](Nb_{1-y}Sb_y)O_3$ ceramics

J.K. Lee [a], J.H. Kim [a], J.H. Cho [b], B.I. Kim [b], E.S. Kim [a,*]

[a] Department of Materials Engineering, Kyonggi University, Suwon 443-760, Republic of Korea
[b] Korea Institute of Ceramic Engineering and Technology, Seoul 153-023, Republic of Korea

Available online 5 May 2011

Abstract

Dependence of electrical properties on the structural characteristics of $Li_{0.04}(K_{0.5}Na_{0.5})_{0.96}(Nb_{1-y}Sb_y)O_3$ (LKNNS ($x = 0$, $0.00 \leq y \leq 0.10$)) and $[Li_{0.04}(K_{0.5}Na_{0.5})_{0.96-x}Ag_x](Nb_{0.925}Sb_{0.075})O_3$ (LKNANS ($0.01 \leq x \leq 0.05$, $y = 0.075$)) were investigated. The oxygen octahedral distortion was dependent on Ag^+ and/or Sb^{5+} content which affected to the phase transition temperature of LKNNS and LKNANS ceramics. The orthorhombic–tetragonal and tetragonal–cubic phase transition temperatures (T_{O-T}, T_C) of the specimens were decreased with increasing of average octahedral distortion. With increasing of Sb^{5+} content, the electromechanical coupling factor (k_p), piezoelectric constant (d_{33}) and dielectric constant (ε_r) of the sintered specimens were increased up to $y = 0.075$, and then decreased. These results could be attributed to the shift of T_{O-T} to near room temperature for $Li_{0.04}(K_{0.5}Na_{0.5})_{0.96}(Nb_{0.0925}Sb_{0.075})O_3$.

Keywords: A. Sintering; C. Electric properties; D. Perovskites; (K,Na)NbO_3

1. Introduction

Lead-free piezoelectric ceramics have been widely investigated to search the environment-friendly replacement for $(Pb,Zr)O_3$ (PZT) ceramics. Although $(K_{0.5}Na_{0.5})NbO_3$ (KNN) ceramics with good electrical properties and high Curie temperature (T_C) were considered as one of the most promising candidates among the lead-free ceramics, KNN ceramics were limited for practical applications due to poor sintered density by the volatility of alkaline elements. Several types of KNN-based ceramics such as KNN–$LiNbO_3$, KNN–$LiSbO_3$ and KNN–$AgNbO_3$ [1] were investigated to improve the sinterability of KNN ceramics, along with the changes of T_C.

Many studies reported that the electrical properties of KNN-based ceramics were improved due to the high alignment of ferroelectric dipoles by orthorhombic to tetragonal phase transition temperature (T_{O-T}) near room temperature [1]. In general, the electrical properties of materials were strongly affected by the structural characteristics as well as T_C and T_{O-T}. Therefore, the dependence of phase transition temperature such as T_C and T_{O-T} on the structural characteristics of KNN-based ceramics should be investigated to control and predict the electrical properties of materials.

It has been reported that KNN-based ceramics shows the structural characteristics such as rattling of cation and octahedral distortion resulted from the substitution of cation with different ionic size for B-site ion in ABO_3 perovskite structure [2].

Therefore, the dependence of electrical properties on the structural characteristics of $[Li_{0.04}(K_{0.5}Na_{0.5})_{0.96-x}Ag_x](Nb_{1-y}Sb_y)O_3$ ceramics were investigated with respect to the phase transition temperatures of T_C and T_{O-T} in this study.

2. Experimental procedures

High-purity oxide powders of K_2CO_3 (99%, High Purity Chemicals, Japan), Na_2CO_3 (99%, High Purity Chemicals, Japan), Li_2CO_3 (99%, High Purity Chemicals, Japan), Nb_2O_5 (99.9%, Sigma–Aldrich, USA), Sb_2O_5 (99.9%, High Purity Chemicals, Japan) and Ag_2O (99%, High Purity Chemicals, Japan) powders were used as the starting powders. The powders were prepared according to the desired composition of $[Li_{0.04}(K_{0.5}Na_{0.5})_{0.96-x}Ag_x](Nb_{1-y}Sb_y)O_3$ ($0.01 \leq x \leq 0.05$, $0.00 \leq y \leq 0.10$) and ground with ZrO_2 balls for 24 h in ethanol. These powders were calcined at 850 °C for 5 h to obtain a single phase. The calcined powders were milled again

* Corresponding author. Tel.: +82 31 249 9764; fax: +82 31 244 6300.
E-mail address: eskim@kyonggi.ac.kr (E.S. Kim).

0272-8842/$36.00
doi:10.1016/j.ceramint.2011.04.115

with ZrO_2 balls for 24 h in ethanol and then dried. Dried powders were pressed isostatically into 10mm-diameter at 1500 kg/cm^2. These pellets were sintered from 1050 °C to 1120 °C for 3 h in air.

Powder X-ray diffraction (XRD, D/Max-3C, Rigaku, Japan) analysis was used to determine the phase identification. The lattice parameters, unit-cell volumes and atomic positions were obtained from Rietveld refinements of XRD patterns using Fullprof [3]. The initial structure model for $(K_{0.5}Na_{0.5})NbO_3$ compounds was taken from the previous reports [4,5]. The parameters such as zero shift, individual scale factor, unit-cell parameters and phase profile parameters (U, V and W) and two asymmetry (orthorhombic and tetragonal) parameters were refined until the apparent convergence of XRD patterns was reached. The microstructure of the specimens was observed using a scanning electron microscope (SEM, JSM-6500F, JEOL, Japan). The vibration of NbO_6 octahedron was confirmed by a Raman spectra meter (T 64000, HORIABA Jobin Yvon, France) with an Ar^+ ion laser operating at 514 nm for excitation.

Silver electrodes were formed on both surfaces of each sintered disk by firing at 700 °C for 10 min. The samples were polarized in silicon oil bath at 120 °C by applying a DC electric field (4 kV mm^{-1} for 20 min). The piezoelectric coefficient (d_{33}) was measured using a piezo-d_{33} meter (ZJ-3BN, Institute of Acoustics, Chinese Academy of Sciences, China). The electromechanical coupling coefficient (k_p) was determined by the resonance and anti-resonance method on the basis of IEEE standards using an impedance analyzer (HP 4192A, Palo Alto, CA, USA). The dielectric constant was measured as a function of temperature by LCR meter (HP 4284A, Agilent, USA).

3. Results and discussion

Fig. 1 shows the XRD patterns of $Li_{0.04}(K_{0.5}Na_{0.5})_{0.96}(Nb_{1-y}Sb_y)O_3$ (LKNNS ($0.00 \le y \le 0.10$)) and/or $[Li_{0.04}(K_{0.5}Na_{0.5})_{0.96-x}Ag_x](Nb_{0.925}Sb_{0.075})O_3$ (LKNANS ($0.01 \le x \le 0.05$))

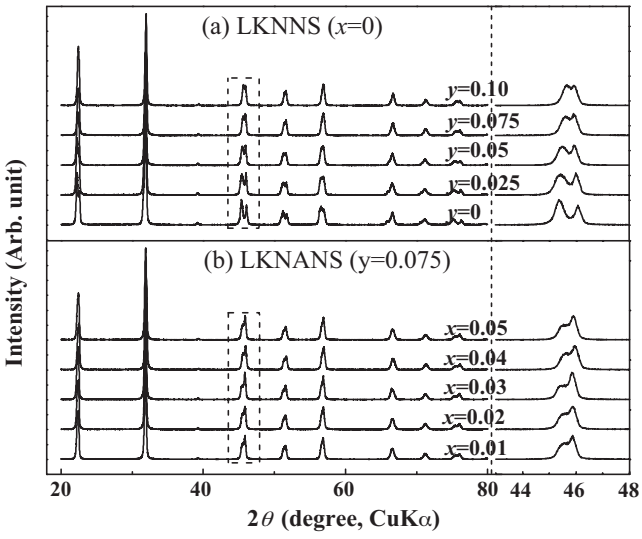

Fig. 1. X-ray diffraction patterns of $[Li_{0.04}(K_{0.5}Na_{0.5})_{0.96-x}Ag_x](Nb_{1-y}Sb_y)O_3$ (LKNNS ($x = 0$, $0 \le y \le 0.1$), LKNANS ($0.01 \le x \le 0.05$, $y = 0.075$)) specimens sintered at 1075 °C for 3 h.

specimens sintered at 1075 °C for 3 h with Sb^{5+} and/or Ag^+ content. A single phase with perovskite structure was detected through the entire range of compositions. The morphotropic phase boundary (MPB) between the orthorhombic (*Amm*2) and tetragonal (*P*4*mm*) phase was detected at 2θ from 43° to 48° for all specimens. The orthorhombic and tetragonal phase of LKNNS were merged with Sb^{5+} content, while those of LKNANS showed the different intensities of those XRD peaks with Ag^+ content. Therefore, the Rietveld refinement procedures were performed to evaluate the structural characteristics in MPB region. Using the two types of the initial structure mode of the orthorhombic (ICSD # 18502) and tetragonal (ICSD # 2852), the lattice parameters and unit-cell volume for each space group were obtained from the Rietveld refinement, as shown in Table 1. The unit-cell volume of each space group was decreased with increasing of Ag^+ and/or Sb^{5+} content. These results are due to the smaller ionic radius of Ag^+ (1.28 Å) than that of K^+ (1.64 Å) and/or Na^+ (1.39 Å) and/or the smaller ionic radius of Sb^{5+} (0.60 Å) than that of Nb^{5+} (0.64 Å) [6]. With increasing of Ag^+ and/or Sb^{5+} content, the volume fraction (V.F.) of orthorhombic phase was decreased, while the V.F. of tetragonal phase was increased. Also, the V.F. of orthorhombic phase of LKNANS was smaller than that of LKNNS, while the V.F. of tetragonal phase of LKNANS was larger than that of LKNNS. From these results, the four types of bond lengths ($2 \times d_1$, $2 \times d_2$, d_3, d_4) for orthorhombic phase and the three types of bond lengths (d_1, d_2, $4 \times d_3$) for tetragonal phase were obtained in NbO_6 octahera, respectively. The octahedral distortion (Δ) of NbO_6 was calculated from the bond length [7]. With increasing of Ag^+ content, the average octahedral distortion (Δ) between orthorhombic and tetragonal phase of LKNANS was decreased up to $x = 0.03$ and then increased. However, the average Δ of LKNNS was increased with Sb^{5+} content.

From the SEM micrographs (not shown), cubic or rectangular morphology of the grain with clear grain boundary could be seen for the specimens with entire range of compositions. With increasing of Sb^{5+} and/or Ag^+ content, the grain size of LKNNS and/or LKNANS ceramics was not changed remarkably. However, the grain size of LKNANS ceramics was larger than that of LKNNS ceramics.

The vibration of NbO_6 octahedron on the $(K_{0.5}Na_{0.5})NbO_3$ (KNN)-based ceramics was determined by the Raman spectrum mode. The Raman spectrum of LKNNS and/or LKNANS ceramics with Sb^{5+} and/or Ag^+ content are showed in Fig. 2. The A_{1g} and F_{2g} modes indicate the double and triply degenerate symmetric O–Nb–O stretching vibration, respectively [7]. In additional, the peaks shift to a lower frequency of A_{1g} and F_{2g} mode means that the distortion of crystal lattice increased due to the larger off-centering of the cation by substitution ion with smaller ionic size.

Fig. 3 shows the temperature dependence of dielectric constant (ε_r) of LKNNS and/or LKNANS ceramics with Sb^{5+} and/or Ag^+ content at 10 kHz, respectively. The temperature dependence of ε_r for the LKNNS ceramics showed two phase transitions, which were corresponded to the orthorhombic–tetragonal phase transition temperature (T_{O-T}) and

Table 1
Refinement results of the crystal structure of $[Li_{0.04}(K_{0.5}Na_{0.5})_{0.96-x}Ag_x](Nb_{1-y}Sb_y)O_3$ (LKNNS ($x = 0$, $0 \le y \le 0.1$), LKNANS ($0.01 \le x \le 0.05$, $y = 0.075$)) specimens sintered at 1075 °C for 3 h.

x (mol)	y (mol)	Space group	Lattice parameter (Å)			$V_{unit\text{-}cell}$ (Å^3)	$\Delta \times 10^4$	[a]V.F.	[b]R_B (%)
			a	b	c				
0.01	0.075	*Amm*2	3.955	5.619	5.645	125.45	51.14	0.49	2.26
		*P*4*mm*	3.960	3.960	3.991	62.57		0.51	2.30
0.02	0.075	*Amm*2	3.955	5.619	5.645	125.44	43.17	0.43	2.16
		*P*4*mm*	3.960	3.960	3.992	62.57		0.57	2.24
0.03	0.075	*Amm*2	3.954	5.614	5.648	125.38	39.10	0.41	2.80
		*P*4*mm*	3.957	3.957	3.957	62.52		0.60	2.38
0.04	0.075	*Amm*2	3.953	5.613	5.646	125.26	42.39	0.37	2.65
		*P*4*mm*	3.958	3.958	3.991	62.53		0.63	2.86
0.05	0.075	*Amm*2	3.954	5.618	5.647	125.46	49.75	0.34	2.58
		*P*4*mm*	3.958	3.958	3.991	62.50		0.66	2.43
0.00	0.00	*Amm*2	3.949	5.680	5.645	126.64	28.51	0.66	3.79
		*P*4*mm*	3.970	3.970	4.008	63.16		0.35	8.39
0.00	0.025	*Amm*2	3.952	5.665	5.639	126.24	29.24	0.63	5.38
		*P*4*mm*	3.964	3.964	4.004	62.93		0.38	8.53
0.00	0.05	*Amm*2	3.953	5.666	5.639	126.32	41.05	0.59	3.77
		*P*4*mm*	3.964	3.964	4.004	62.92		0.41	8.49
0.00	0.075	*Amm*2	3.955	5.625	5.641	125.51	51.69	0.51	3.53
		*P*4*mm*	3.963	3.963	3.993	62.71		0.49	2.93
0.00	0.10	*Amm*2	3.955	5.634	5.635	125.57	64.77	0.51	2.67
		*P*4*mm*	3.963	3.963	3.988	62.62		0.49	5.95

[a] Volume fraction.
[b] Bragg R-factor.

tetragonal–cubic phase transition temperature (T_C). Although the T_C of LKNNS was decreased with Sb^{5+} content, the T_{O-T} was shifted to near room temperature up to $y = 0.075$ and then that disappeared with further addition of Sb^{5+}. However, the T_{O-T} of LKNANS was not observed and the T_C was not changed remarkably with Ag^+ content. These results could be attributed to the average oxygen octahedral distortion, as shown in Fig. 4. With increasing of average octahedral distortion Δ, the T_C, T_{O-T} of LKNNS and T_C of LKNANS were decreased, while the decrease of T_C with Δ for LKNNS was larger than that of LKNANS. These results are due to the fact that the relative amount of orthorhombic phase to tetragonal phase of LKNNS in MPB region was larger than that of LKNANS, as confirmed in Fig. 1.

Fig. 5 show the piezoelectric constant (d_{33}), electromechanical coupling coefficient (k_p) and dielectric constant (ε_r) of the

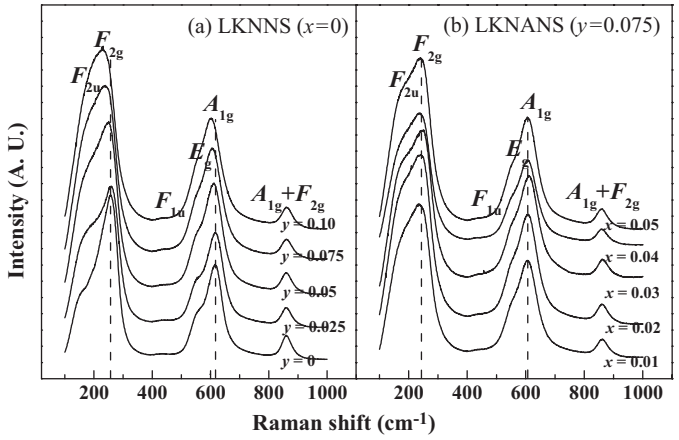

Fig. 2. Raman spectrum of $[Li_{0.04}(K_{0.5}Na_{0.5})_{0.96-x}Ag_x](Nb_{1-y}Sb_y)O_3$ LKNNS ($x = 0, 0 \le y \le 0.1$), LKNANS ($0.01 \le x \le 0.05$, $y = 0.075$) specimens sintered at 1075 °C for 3 h.

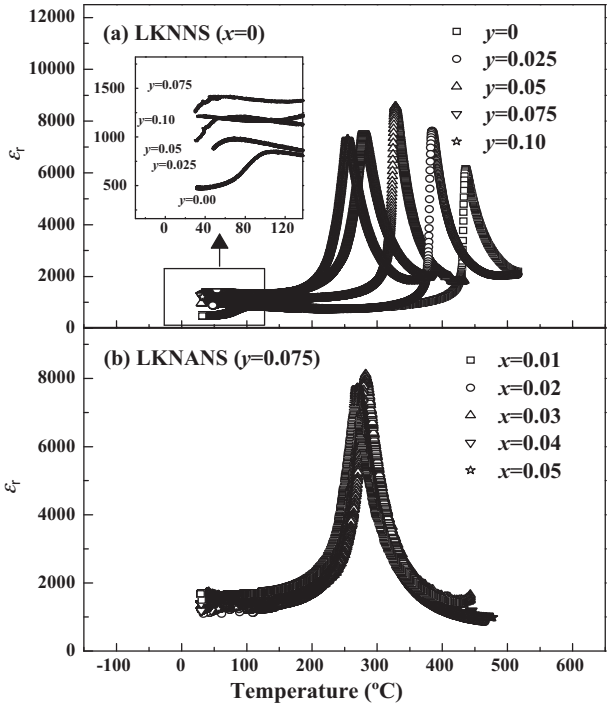

Fig. 3. Temperature dependence of the dielectric constant (ε_r) for $[Li_{0.04}(K_{0.5}Na_{0.5})_{0.96-x}Ag_x](Nb_{1-y}Sb_y)O_3$ (LKNNS ($x = 0$, $0 \le y \le 0.1$), LKNANS ($0.01 \le x \le 0.05$, $y = 0.075$)) specimens sintered at 1075 °C for 3 h.

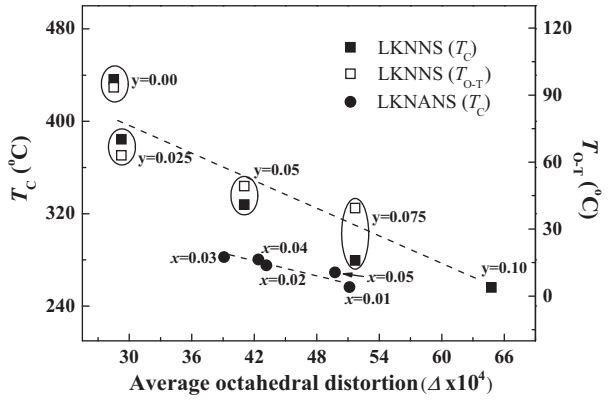

Fig. 4. Dependence of phase transition temperature on the average oxygen octahedral distortion for $[Li_{0.04}(K_{0.5}Na_{0.5})_{0.96-x}Ag_x](Nb_{1-y}Sb_y)O_3$ (LKNNS ($x = 0$, $0 \le y \le 0.1$), LKNANS ($0.01 \le x \le 0.05$, $y = 0.075$)) specimens sintered at 1075 °C for 3 h.

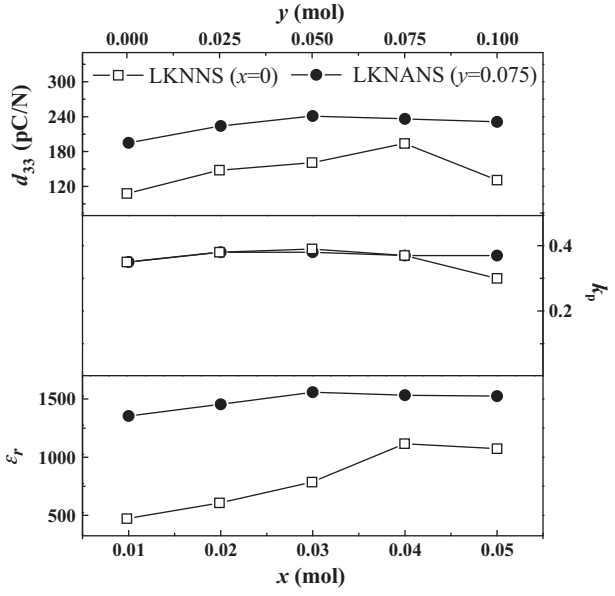

Fig. 5. Electrical properties (d_{33}, k_p and ε_r) of $[Li_{0.04}(K_{0.5}Na_{0.5})_{0.96-x}Ag_x](Nb_{1-y}Sb_y)O_3$ (LKNNS ($x = 0$, $0 \le y \le 0.1$), LKNANS ($0.01 \le x \le 0.05$, $y = 0.075$)) specimens sintered at 1075 °C for 3 h.

LKNNS and/or LKNANS ceramics with Sb^{5+} and/or Ag^+ content. With increasing of Sb^{5+} content, the d_{33} and ε_r of LKNNS ceramics increased up to $y = 0.075$ due to the T_{O-T} near room temperature (Fig. 3) [1] and rattling effect [2] of cation by substitution of Sb^{5+} for Nb^{5+} and then decreased, while the k_p was not changed remarkably. Although the d_{33}, k_p, and ε_r of LKNANS ceramics were not changed remarkably with Ag^+ content, the d_{33} and ε_r of LKNANS ceramics were larger than those of LKNNS ceramics. These results could be explained that the T_{O-T} of LKNANS ceramics was more shifted toward room temperature than that of LKNNS ceramics.

4. Conclusions

For the $Li_{0.04}(K_{0.5}Na_{0.5})_{0.96}(Nb_{1-y}Sb_y)O_3$ (LKNNS ($0.00 \le y \le 0.10$)) and $[Li_{0.04}(K_{0.5}Na_{0.5})_{0.96-x}Ag_x](Nb_{0.925}Sb_{0.075})O_3$(LKNANS ($0.01 \le x \le 0.05$)) specimens sintered at 1075 °C for 3 h, morphotrophic phase boundary (MPB) between orthorhombic and tetragonal phase was detected through the entire range of compositions. With increasing of Ag^+ and/or Sb^{5+} content, the volume fraction of tetragonal phase was increased. The phase transition temperature (T_{O-T}, T_C) was decreased with increasing of average oxygen octahedral distortion. Typically, $d_{33} = 194$pC/N, $k_p = 0.37$ and $\varepsilon_r = 1116$ for $Li_{0.04}(K_{0.5}Na_{0.5})_{0.96}(Nb_{0.925}Sb_{0.075})O_3$ and $d_{33} = 241$pC/N, $k_p = 0.38$ and $\varepsilon_r = 1533$ for $[Li_{0.04}(K_{0.5}Na_{0.5})_{0.93}Ag_{0.03}](Nb_{0.925}Sb_{0.075})O_3$ were obtained for the specimens sintered at 1075 °C for 3 h.

Acknowledgement

This research was supported by a grant from the Fundamental R&D Program for Core Technology of Materials funded by the Ministry of Knowledge Economy, Republic of Korea.

References

[1] J. Rodel, W. Jo, K.T.P. Seifert, E.M. Anton, T. Granzow, D. Damganovic, Perspective on the development of lead-free piezoceramics, Journal of the American Ceramic Society 92 (6) (2009) 1153–1177.
[2] E.S. Kim, B.S. Chun, D.H. Kang, Effects of structural characteristics on microwave dielectric properties of $(1-x)Ca_{0.85}Nd_{0.1}TiO_3-xLnAlO_3$ (Ln = Sm, Er and Dy) ceramics, Journal of the European Ceramic Society 27 (2007) 3005–3010.
[3] T. Roisnel, J.R. Carvajal, WinPLOTR: a windows tool for powder diffraction patterns analysis, Materials Science Forum 378–381 (2001) 118–123.
[4] L. Katz, H.D. Megaw, The structure of potassium niobate at room temperature: the solution of a pseudosymmetric structure by Fourier methods, Acta Crystallographica 22 (1967) 639–648.
[5] A.M. Glazer, H.D. Megaw, The Structure of Sodium Niobate (T_2) an 600 °C, and the Cubic–Tetragonal Transition in Relation to Soft-phonon Modes, vol. 1, Golden Book of Phase Transitions, Wroclaw, 2002, pp. 1–123.
[6] R.D. Shannon, Revised effective ionic radii and systematic studies of interatomic distances in halides and chalcogenides, Acta Crystallographica A32 (1976) 751–767.
[7] H.R. Xia, H.C. Chen, H. Yu, K.X. Wang, B.Y. Zhao, Vibrational spectra of a $K_{0.30}Na_{0.10}Sr_{0.48}Ba_{0.32}Nb_2O_6$ single crystal studied by Raman and infrared reflectivity spectroscopy, Physica Status Solidi (b) 210 (1998) 47–59.